

PDA: Progressive Data Augmentation for General Robustness of Deep Neural Networks

Hang Yu^{*1}, Aishan Liu^{*1}, Xianglong Liu^{†1}, Gengchao Li¹, Ping Luo²,
Ran Cheng³, Jichen Yang¹, and Chongzhi Zhang¹

¹State Key Laboratory of Software Development Environment, Beihang University

²The University of Hong Kong

³Southern University of Science and Technology

Abstract

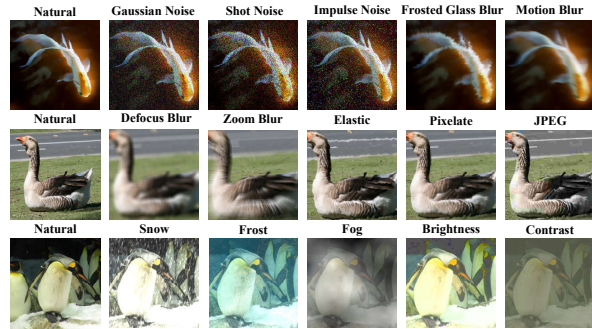
Adversarial images are designed to mislead deep neural networks (DNNs), attracting great attention in recent years. Although several defense strategies achieved encouraging robustness against adversarial samples, most of them fail to improve the robustness on common corruptions such as noise, blur, and weather/digital effects (e.g. frost, pixelate). To address this problem, we propose a simple yet effective method, named Progressive Data Augmentation (PDA), which enables general robustness of DNNs by progressively injecting diverse adversarial noises during training. In other words, DNNs trained with PDA are able to obtain more robustness against both adversarial attacks as well as common corruptions than the recent state-of-the-art methods. We also find that PDA is more efficient than prior arts and able to prevent accuracy drop on clean samples without being attacked. Furthermore, we theoretically show that PDA can control the perturbation bound and guarantee better generalization ability than existing work. Extensive experiments on many benchmarks such as CIFAR-10, SVHN, and ImageNet demonstrate that PDA significantly outperforms its counterparts in various experimental setups.

1. Introduction

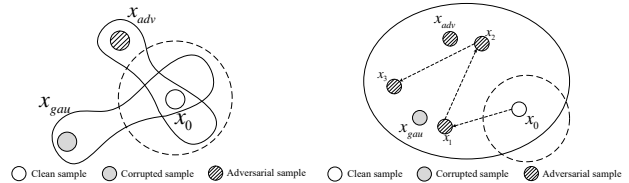
Recent advanced deep neural networks (DNNs) achieve great successes in many fields including computer vision [19], natural language processing [2], and speech processing [17]. Their performances are typically obtained by training with sufficient amount of ‘clean’ data. However,

^{*}Contribute Equally.

[†]Corresponding author.



(a) Some corrupted images in ImageNet-C



(b) PGD & GDA

(c) PDA

Figure 1. An illustration of corrupted images (a) and the classification of models with PGD, GDA (b) and PDA (c). For both (b) and (c), the dashed curves represent the decision boundary of naturally trained models. Without covering the adversarial and corrupted samples promises better clean accuracy but almost no robustness. The solid curves denote the decision boundary after trained with augmented data. For PGD & GDA (b), the decision space is “stretched” after augmentation (e.g. x_{adv} and x_{gau}) in some specific orientations, which causes the accuracy drop on clean samples. However, for our PDA (c), more diversified data are computed, aggregated and injected (e.g. x_1, x_2, \dots) in various directions, which enlarges the decision space to cover adversarial, corrupted and clean samples simultaneously. The larger decision space of PDA promises the general robustness and prevents the drop of clean accuracy. In CIFAR-10, SVHN and ImageNet, PDA has comparable adversarial robustness and around 3% above on clean accuracy when compared with PGD. In CIFAR-10-C and ImageNet-C, PDA has about 10% above on mean Corruption Error (mCE) when compared with GDA.

in real-world scenario, the training and test data may contain many types of noises. For example, adversarial images (*e.g.* adversarial sample generated by injecting small perturbation in an input image of DNN) and image corruptions [16] such as noise, blur, and weather/digital effects (*e.g.* frost, pixelate) have been proven to threaten performance of DNNs [22, 20], making them un-robust when deploying in scenarios that demand high security. This work intends to well understand and improve robustness of DNNs when significant adversarial samples and corruptions are presented. In the recent years, many efforts have been devoted to improve robustness of DNNs in terms of *attack* [13, 1] and *defense* [36, 21, 24]. The attack approaches aim to inject noises or adversarial samples to confuse a DNN, while the defense approaches aim at preventing DNNs from being attacked. The existing work can be generally categorized into two streams. In the first stream, the defense methods attempt to build DNNs with adversarial robustness by gradient masking. Some of the defenses make classifier learn to break gradient descent, others are designed to purposely cause gradient masking as obfuscated gradients. Although they obtained certain stabilization for DNNs when adversarial samples are presented, for those methods designed to obfuscate gradients, they still could be easily circumvented by constructing function to approximate the non-differentiable layer on the backward pass, or by approximating the expectation with samples over the transformation to correctly compute the gradient [1]. The recently proposed *adversarial training* appears a strong defense algorithm by using adversarial data augmentation, showing strong capability to train robust DNNs against adversarial samples. However, training on one-step adversarial examples does not confer robustness to iterative white-box attack [20] at ImageNet scale. It is possible that much larger models are necessary to achieve robustness to such a large class of inputs.

In the second stream, recent studies have paid attention to improve model robustness against common corruptions [41, 34]. For example, corruptions like Gaussian blur and noise would greatly impede performance of DNNs as shown in [9, 16]. Although the above work achieved certain progress, they mainly focused on defending either corruptions [41, 34] or adversarial samples [21, 24], but seldom work have devoted to defend both of them. For example, only a few pioneering work [11, 10, 12] try to establish relationship between adversarial samples and random noises (*e.g.* additive Gaussian noise), leading to more general robustness of DNNs. It remains an open question to build strong DNNs that are able to against both adversarial samples and image corruptions by using a unified framework.

To understand DNNs' robustness and bridge the above gap, this work devises a novel algorithm, named *Progressive Data Augmentation (PDA)*, which is a unified framework to improve robustness of DNNs against both adversar-

ial samples and corruptions including noises, blur, weather and digital effects. PDA is significantly different from prior arts that achieved robustness by using large-scale additional training data [28, 33]. Instead of simply augmenting data, PDA explores an alternative perspective by progressively aggregating, augmenting, and injecting adversarial noises during adversarial training. We prove that PDA is beneficial to improve robustness against both adversarial samples and corruptions. For example, we show that PDA is able to satisfy the perturbation bound and guarantee better generalization ability. Furthermore, extensive experiments on multiple datasets including CIFAR-10 [18], SVHN [26], ImageNet [8], CIFAR-10-C [16] and ImageNet-C [16] demonstrate that PDA outperforms existing approaches in various experimental settings.

1.1. Related Work

Adversarial Robustness. Many adversarial training based methods have been proposed to improve model robustness against adversarial examples. [24] trained robust model with the PGD augmented adversarial samples, whereas it consumes too much time and fails to generalize well on clean examples. Meanwhile, [32] proposed a provable adversarial training algorithm with a surrogate loss, but it is only confined to the small dataset, *e.g.* MNIST. Besides, [27] calculated and added adversarial noises to each hidden layer during training to tackle the overfitting problem. Moreover, [29] and [40] both brought efficient strategies on the conventional adversarial training algorithm to achieve adversarial robustness without much time cost. However, seldom work achieved the robustness in more general situations (*e.g.* corruptions), and the adversarial training based method still remains questionable to various corrupted samples.

Corruption Robustness. When it comes to training the robust model towards corrupted samples, rare effective approaches have been proposed. [41] utilized stability training to stabilize model behavior against small input distortions, and [34] employed feature quantization techniques to deal with distorted images such as motion blur, salt and pepper. [25] drew insights from meta-learning which uses a learned optimizer to build a robust model against input noises (*e.g.* translations). [12] found the positive correlation between adversarial and corruption robustness. However, the Gaussian data augmentation they used only has limited improvement on adversarial robustness. More recently, [23] devised patch Gaussian augmentation method to improve the corruption robustness with little side effects on clean accuracy, yet the performance on adversarial robustness was not provided in this work.

Data Complexity and Diversity. Prior studies [28, 33] have shown that the sample complexity plays a critical role in training a robust deep model. [28] concluded that the

sample complexity of robust learning can be significantly larger than that of standard learning under adversarial robustness situation. [7] believed that adversarial training may need exponentially more iterations to obtain large margins compared to standard training. Moreover, [39] theoretically and empirically showed that with more unlabeled data, the model can be learned with better adversarial robust generalization.

2. Background and Notation

In this section, we provide the definitions of the adversarial robustness and corruption robustness, taking the widely studied and used convolutional neural networks in image classification as the basic deep models. Given a training sample $x \in \mathcal{X}$ and label $y \in \mathcal{Y}$, the pair of (x, y) from distribution D , the deep supervised learning model tries to learn a function $f: \mathcal{X} \rightarrow \mathcal{Y}$ as the mapping from input examples to output labels. Specifically, we use log-loss in the image classification problem:

$$\ell(\theta; x, y) = - \sum_{i=1}^m y_i \log \left(\frac{e^{f(\theta; x, y_i)}}{\sum_{j=1}^m e^{f(\theta; x, y_j)}} \right),$$

where θ denotes the parameter of a given neural network, and $f(\theta; x, y_i)$ is the score given to the pair (x, y_i) by a function f .

Specifically, **adversarial robustness** is defined as $\min_{\|\delta\|_p \leq \varepsilon} \mathbb{P}_{(x,y) \sim D}(f(x + \delta) = y)$, i.e., the probability of right classification when a random sample from distribution D is perturbed by the small adversarial noise δ controlled by ε ; and **corruption robustness** is defined as $\mathbb{P}_{(x,y) \sim D}(f(c(x)) = y)$, i.e., the probability of right classification when a sample from distribution D is corrupted by the transformation function $c(\cdot)$ [16].

Generally, the adversarial attack by generating adversarial examples can be defined as:

$$x' = \arg \max_{\|x' - x\|_p \leq \varepsilon} \ell(\theta; x, y),$$

where ε represents the perturbation magnitude. The optimization process could be approximately solved with the first-order expansion [30]:

$$x' = \arg \max_{\|x' - x\|_p \leq \varepsilon} \nabla_x (\ell(\theta; x, y))^T (x' - x).$$

In the case $p = \infty$, we obtain $x' = x + \varepsilon \text{sign}(\nabla_x \ell(\theta; x, y))$, which is the famous attack Fast Gradient Sign Method (FGSM [14]). The iterative version of this generating process are proposed by [20] and [24], which obtains stronger adversarial examples.

To enhance adversarial robustness, the **adversarial training** can be performed by solving:

$$\min_{\theta} \mathbb{E}_{(x,y) \sim D} \max_{\|\delta\|_p \leq \varepsilon} \ell(\theta; x + \delta, y),$$

where the process can be regarded as the augmentation of x with the adversarial example $x + \delta$ in the normal training. Among various attack methods, the projected gradient descent (PGD) [24] is commonly used in the adversarial training as PGD-AT to achieve excellent adversarial robustness. However, the searching process of δ in PGD requires massive computation cost, which motivates us to propose an efficient method to achieve comparable adversarial robustness.

A common idea for enhancing the corruption robustness is to add Gaussian noise in the training process:

$$\min_{\theta} \mathbb{E}_{(x,y) \sim D} \ell(\theta; x + \mathcal{N}(x; \sigma^2 I), y),$$

where the training process could be regarded as the Gaussian data augmentation (GDA) [12]. Despite of its simple implementation, GDA only has limited performance against adversarial examples and other corruptions beyond noise.

3. Progressive Data Augmentation (PDA)

From the data complexity point of view [28, 33, 39], we introduce an adversarial-based method called *Progressive Data Augmentation (PDA)*. During multiple iterations within each training step, PDA adds adversarial noises progressively with different magnitudes into training data. Different from PGD or GDA, our progressive data augmentation significantly increases the data diversity with more flexible perturbations during each training step. Therefore, the models trained with PDA are expected to be generally more robust against more types of noises, including both adversarial examples and corruptions. Moreover, the process of generating augmented noises could be significantly faster than PGD-based method as it merely utilizes the training gradients with little extra computation cost. Therefore, in comparison with the searching process of PGD-based methods, PDA is more efficient in generating diversified noises.

The surrogate loss was first proposed in [32], by adding the Lagrangian constraint to the original loss function to approximate the worst-case perturbation. Analogously, we can update the model parameter θ and δ by minimizing the following surrogate loss:

$$\ell_{\lambda}(\theta; x, y) = \min_{\theta} \sup_{\delta} [\ell(\theta; x, y, \delta) - \frac{\lambda}{2} \|\delta\|_2^2], \quad (1)$$

where δ represents the added perturbation which helps approximate the objective robust distribution.

Specifically, given a pair of training samples (x, y) , we assume δ as the perturbation to be updated with gradient ascent. Since data complexity contributes significantly to adversarially robust model, we propose a progressive iteration process to introduce diversified adversarial examples. Given the fact that $k \|\nabla_{\delta} \ell(\theta; x, y, \delta)\|_2 = k \|\nabla_{\delta} \ell(\theta; x, y, \delta)\|_2$

and $\nabla_{\delta} \ell_{\lambda}(\theta; x, y) = \nabla_{\delta} \ell(\theta; x, y, \delta) - \lambda \|\delta\|_2$, we have

$$\delta \leftarrow \delta + \frac{\varepsilon}{\|k \nabla_{\delta} \ell(\theta; x, y, \delta)\|_2} \cdot \nabla_{\delta} \ell_{\lambda}(\theta; x, y), \quad (2)$$

Thus, the perturbation δ could be updated in every step j during the progressive process as:

$$\delta^j \leftarrow (1 - \lambda) \delta^{j-1} + \frac{\varepsilon}{k} \cdot \frac{\nabla_{\delta^{j-1}} \ell(\theta; x^{j-1}, y, \delta^{j-1})}{\|\nabla_{\delta^{j-1}} \ell(\theta; x^{j-1}, y, \delta^{j-1})\|_2}, \quad (3)$$

where λ corresponds to the l_2 regularization factor and the magnitude ε is normalized by the number of steps k , such that the overall magnitude of update equals ε . λ here controls perturbation decay with the increase of progressive iterations as well as the contribution of the former perturbation δ^{j-1} . Then we augment the current training sample as $x^j \leftarrow x^{j-1} + \delta^j$, and update model parameter with the augmented x^j , progressively.

In the training epoch t we diversified the overall perturbation magnitude ε^t as $\{0, \frac{\varepsilon}{3}, \frac{\varepsilon}{2}, \varepsilon, \frac{\varepsilon}{2}, \frac{\varepsilon}{3}, 0\}$. For the first half of training process, the ascent of magnitude is similar to the curriculum learning [3], which makes the model easier to learn. For the second half of training epochs, the descent of magnitude could help fix the decision boundary and make it smoother, which is beneficial to the classification of benign samples.

Algorithm 1 Progressive Data Augmentation

Require: Training set $\{(x_i, y_i)\}_{i=1}^n$, Hyper-parameters λ , ε , k , learning rate η

Ensure: Updated model parameters θ

- 1: **for** t in T epochs **do**
 - 2: $\varepsilon^t \in \{0, \frac{\varepsilon}{3}, \frac{\varepsilon}{2}, \varepsilon, \frac{\varepsilon}{2}, \frac{\varepsilon}{3}, 0\}$, for diversification
 - 3: **for** j in k iterative steps **do**
 - 4: $\delta^j \leftarrow (1 - \lambda) \delta^{j-1} + \frac{\varepsilon^t}{k} \cdot \frac{\nabla_{\delta^{j-1}} \ell(\theta; x^{j-1}, y, \delta^{j-1})}{\|\nabla_{\delta^{j-1}} \ell(\theta; x^{j-1}, y, \delta^{j-1})\|_2}$
 - 5: $x^j \leftarrow x^{j-1} + \delta^j$
 - 6: $\theta \leftarrow \theta - \eta \nabla_{\theta} \ell(\theta; x^j, y, \delta^j)$
 - 7: **end for**
 - 8: **end for**
-

4. Theoretical Analysis

Now, we further analyse the possible perturbation bound with respect to robustness and the upper bound on the expected generalization error. For the loss function $\ell(\theta; x, y)$, obviously there exist upper bounds M_0 and M_1 , such that $|\ell(\theta; x, y)| \leq M_0$ and $\|\nabla_x \ell(\theta; x, y)\|_2 \leq M_1$.

Assuming that the loss function is smooth, there exist L_0 and L_1 such that $|\ell(\theta; x, y) - \ell(\theta; x', y')| \leq L_0 \|x - x'\|_2$, $\|\nabla_x \ell(\theta; x, y) - \nabla_x \ell(\theta; x', y')\|_2 \leq L_1 \|x - x'\|_2$, where (x, y) and (x', y') denote two pairs of samples.

Perturbation Bound. We set $z = g(\theta; x)$ as the mapping from the input x to the output of last hidden layer z . By defining the output set of z as \mathcal{Z} and rewriting $\ell(\theta; x, y)$ as $\ell(\theta; z, y)$ with the variable z , we define z_{ε}^* as the ε -maximizer [4] of $\ell(\theta; z, y)$: $z_{\varepsilon}^* \in \varepsilon - \arg \max_{z \in \mathcal{Z}} \{\ell(\theta; z, y)\}$. Given a pair of sample (x_0, y_0) , z_0 denotes the output of last hidden layer for sample x_0 . Then we have:

Theorem 1 *In the intersection U of the neighborhoods of z_0 and $z_0 - (\nabla_{zz} \ell(\theta; z_0, y_0))^{-1} \nabla_z \ell(\theta; z_0, y_0)$, we assume:*

1. *There exists C , s.t. $\forall z \in U$, $\|\nabla_{zz} \ell(\theta; z, y)\|_2 \geq C$;*
2. *There exists K , s.t. $\forall z \in U$, $\|(\nabla_z \ell(\theta; z, y_0) - \nabla_z \ell(\theta; z_0, y_0)) - \nabla_{zz} \ell(\theta; z_0, y_0)(z - z_0)\|_2 \leq K$.*

With the above assumptions, we have the perturbation bound as follows:

$$\|z_{\varepsilon}^* - z_0\|_2 \leq \frac{K}{C} + \sqrt{\frac{\varepsilon}{C} + \|(\nabla_{zz} \ell(\theta; z_0, y_0))^{-1} \nabla_z \ell(\theta; z_0, y_0)\|_2}$$

The detailed proof of Theorem 1 can be found in the appendix. With the definition of ε -maximizer and the above assumptions, we are able to find the proper space in some neighborhood to satisfy the conditions, and thus compute the output range of the last hidden layer. Therefore, with Theorem 1, we could estimate the impact of adversarial examples and the potential risk with the distance between the worst-case perturbed one and the normal one.

Generalization Ability Bound. Specifically, we denote $N(\gamma, \mathcal{X}, \|\cdot\|_p)$ as the covering number of \mathcal{X} using γ -balls for $\|\cdot\|_p$. Inspired by the Theorem 3 in [37], we have:

Theorem 2 *Given augmented training set \mathcal{X} , for any probability $p > 0$, there is at least probability $1 - p$ such that surrogate loss satisfies*

$$\begin{aligned} \ell_{\lambda}(\theta; x, y) &\leq \frac{1}{n} \sum_{i=1}^n \hat{\ell}(\theta; x, y) + \gamma(L_0 + \frac{2M_1 L_1 + 1}{\lambda}) \\ &+ M_0 \left(\sqrt{\frac{2N(\gamma/2, \mathcal{X}, \|\cdot\|_2) \ln 2 - 2 \ln p}{n}} \right) + \frac{M_1^2}{\lambda - L_1}, \end{aligned}$$

where $n = |\mathcal{X}|$ denotes the volume of training set and $\hat{\ell}$ denotes the empirical training loss.

Furthermore, the theoretical analyses of generalization error upper bound for the surrogate loss of PDA can be found in the appendix. Let us denote the Lipschitz constant of $\ell_{\lambda}(\cdot)$ as $L_{\lambda} = L_0 + \frac{2M_1 L_1 + 1}{\lambda}$, then the difference between losses could be constrained in γL_{λ} with similar input examples, and there is a balance between the covering number $N(\gamma/2, \mathcal{X}, \|\cdot\|_2)$ and γL_{λ} . If γ increases, then the former covering number decreases and γL_{λ} increases

at the same time, which promises a reasonable generalization bound with the robust property. Therefore, according to Theorem 2, PDA could build robust model with proved upper bound on the generalization error.

5. Experiments

In this section, we will evaluate our *Progressive Data Augmentation* and other strategies on the image classification task against adversarial and corrupted examples.

We adopt the popular **CIFAR-10** [18], **SVHN** [26] and **ImageNet** [8] as the evaluation datasets of adversarial robustness. As for the deep models, we choose the widely-used models, VGG16 [31] and Wide ResNet34 for CIFAR-10, standard ResNet18 [15] for SVHN and AlexNet [19] for ImageNet respectively. For simplicity, we only choose 200 out of the 1000 classes in ILSVRC-2012 with 100K images for training set and 10k for validation set. All experiments are taken on the single NVIDIA Tesla V100 GPU.

For the experiments of corruption robustness, we evaluate our proposed method on the benchmark [16] **CIFAR-10-C** and **ImageNet-C**. CIFAR-10-C and ImageNet-C are the first datasets for benchmarking model robustness against different common corruptions with different severity levels. They are created from the test set of CIFAR-10 and validation set of ImageNet. There are 15 kinds of corruptions in the dataset we have used, comprising the sets of Noise, Blur, Weather and Digital. Specifically, Noise contains {Gaussian, Shot, Impulse}, Blur contains {Defocus, Glass, Motion, Zoom}, Weather contains {Snow, Frost, Fog, Bright}, Digital contains {Contrast, Elastic, Pixel, JPEG}. Each corruption has 5 severities.

For the experiments of adversarial robustness in CIFAR-10 and SVHN, we evaluate the augmented model with Projected Gradient Descent (**PGD** [24]) on l_{inf} norm and the **C&W** attack [6] on l_2 norm. The *PGD-k* attack means the PGD attack with iteration steps k . For PGD attack, we set the overall magnitude of perturbation ϵ as 4/255, 8/255 and 12/255 (4,8,12 for short) respectively, and set the iteration steps $k=20$. For C&W attack, we set the l_2 perturbation size $c=500$, which is similar to [40]. For ImageNet, we evaluate the models with PGD-20 attack and BPDA [1] attack, where the perturbation magnitude $\epsilon=8/255$ (8 for short).

For CIFAR-10, SVHN and ImageNet, we evaluate the performance of model with our progressive data augmentation (**PDA**), compared with naturally trained model (**Naturally Trained** or **Natural** for short), model with projected gradient descent (**PGD**) and model with Gaussian data augmentation (**GDA** [12]). We use *PGD-k- α* to represent the model augmented by PGD with iteration steps k and attack step size α , where we set $k=5$ or 10 and $\alpha=1/255$ (1 for short). We use *GDA- σ* to represent the model augmented by Gaussian noise $\mathcal{N}(\cdot; \sigma^2 I)$, where we set $\sigma=0.1$ or 0.4 in the training process. For our method, we use *PDA-*

k- ϵ to represent the model augmented by more varied noise with perturbation magnitude ϵ and iteration times k .

5.1. Evaluation Criteria

For adversarial robustness, we evaluate the model robustness with top-1 classification accuracy on adversarial datasets. For corruption robustness, [16] proposed some different metrics to score the performance of a classifier, which could comprehensively evaluate a classifier’s robustness to corruption.

Given a trained classifier f which has not been trained on corruption set, we compute the top-1 error rate on clean images as E_{clean}^f . Then we test the classifier on each corruption c at each level of severity s , denoted as $E_{s,c}^f$, and divide by the error rate of baseline $E_{s,c}^{base}$ for adjustment. Finally, the mean Corruption Error (**mCE**) is computed as:

$$CE_c^f = \frac{\sum_{s=1}^5 E_{s,c}^f}{\sum_{s=1}^5 E_{s,c}^{base}},$$

which means the average of 15 different Corruption Errors (CE). Moreover, the amount that the classifier declines on corrupted inputs can be measured with **Relative mCE**. (RmCE for short). If a classifier withstands the most corruption, the gap between mCE and the clean error rate is minuscule. Thus, Relative mCE is calculated as:

$$RmCE_c^f = \frac{\sum_{s=1}^5 E_{s,c}^f - E_{clean}^f}{\sum_{s=1}^5 E_{s,c}^{base} - E_{clean}^{base}}.$$

5.2. Adversarial Robustness

CIFAR-10 We conduct the experiments of adversarial robustness on CIFAR-10 to demonstrate the effectiveness of our proposed PDA. Table 1 shows that PDA achieves state-of-the-art results on both of these adversarial attack benchmarks. Besides the performance against adversarial attacks, we could notice that diversified noises augmented in training data remarkably improve the model performance on clean images, as illustrated in Figure 1. With the increase of perturbation magnitude for these augmentation strategies, there is a trade-off between clean accuracy and adversarial performance, indicating that our PDA is more suitable in the general case. We further compare the computation cost of PDA with PGD on VGG16 and CIFAR-10. As indicated by the results in Table 2, PDA is computationally more efficient than PGD in the same training epochs.

Similarly, we compare our PDA method with other two current methods ‘Free-m’ [29] and ‘YOPO’ [40]. YOPO compared the while-box PGD-20 attack performance and time consumption with Free-m using Wide ResNet34 on CIFAR-10. As shown in Table 3, PDA achieves comparable performance on adversarial attack with less time cost. Compared with other augmented strategies, PDA still has

Table 1. The adversarial robustness of naturally trained model and models with PGD, GDA and PDA using VGG16 on CIFAR-10. Following the guidelines from [5], models are evaluated with the gradient-based attack (PGD) in l_{inf} norm and optimization-based attack (CW) in l_2 norm. PDA performs comprehensively well on adversarial attack as well as clean images.

VGG16	Clean	PGD-20 Attack ($\epsilon=8, 12$)		CW Attack ($c=500$)
Natural	92.52%	0.17%	0.00%	6.72%
PGD-5-1 [24]	87.60%	44.78%	28.03%	45.01%
GDA-0.1 [12]	89.14%	11.61%	2.05%	55.15%
PDA-3-1.0	90.94%	41.06%	25.08%	67.17%
PDA-3-2.0	89.56%	44.87%	33.91%	55.19%

Table 2. The time consumption of training process with VGG16 on CIFAR-10. PDA achieves 1/6 to 1/5 computation cost of PGD.

Time cost (mins) for 80 epochs	PGD-5-1 [24]	PDA-3-2.0
VGG16	174.424	30.572

Table 3. The adversarial robustness and time cost of Wide ResNet34 using different strategies on CIFAR-10. PDA achieves comparable adversarial performance and computation cost as well as better clean accuracy compared with its counterparts.

Wide ResNet34	Clean	PGD-20 Attack	Time Cost (mins)
Natural	95.03%	0.00%	233
PGD-10 [24]	87.30%	47.04%	2713
Free-8 [29]	86.29%	47.00%	667
YOPO-5-3 [40]	86.70%	47.98%	476
PDA-3-16	89.12%	48.14%	408

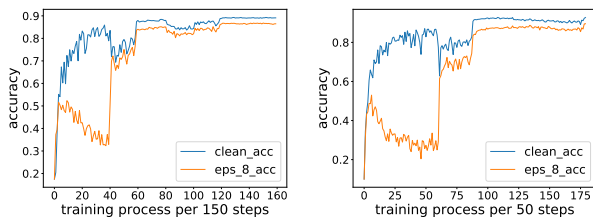


Figure 2. The change of accuracy in the training process of model with PDA using VGG16 (left) and Wide ResNet34 (right) on CIFAR-10. The blue curve represents clean accuracy and the orange curve denotes the performance against black-box adversarial examples by PGD-20 attack ($\epsilon=8/255$).

better accuracy on clean images due to more varied data in augmentation.

In Figure 2, we provide the accuracy curves using PDA in the training process on CIFAR-10. For the model with PDA strategy, the additive noises are diversified in many phases. In the first drop of orange curve ('eps_8_acc') without additive noise of PDA, we could notice that the adversarial robustness starts to decrease after a period of increase, while the clean accuracy keeps increasing. This can be attributed

to the roughness of decision boundary and the tendency of overfitting. After more varied data is augmented, the black-box adversarial robustness tends to increase in accordance with the clean accuracy.

SVHN We use standard ResNet18 model to evaluate the adversarial robustness on SVHN. Due to the lack of related corruption set, we only test the adversarial performance of models. Table 4 shows that our PDA achieves better performance on both adversarial attack and clean images, in comparison with other augmentation strategies.

Table 4. The results of adversarial robustness for ResNet18 on SVHN. The attack step size α of PGD-20 attack is the same as CIFAR-10. PDA performs better than PGD and GDA against adversarial attack as well as clean images.

ResNet18	Clean	PGD-20 Attack ($\epsilon=4, 8$)		CW Attack ($c=500$)
Natural	96.42%	43.51%	10.37%	8.89%
PGD-10-1 [24]	93.23%	64.56%	38.30%	19.70%
GDA-0.1 [12]	94.72%	59.62%	30.74%	16.11%
PDA-3-1.0	96.11%	72.34%	47.08%	21.58%

ImageNet Due to the limited space of device, we randomly select 200 out of the 1000 classes of original ImageNet, and restrict the training set as 100k and the validation set as 10k. We use AlexNet to evaluate the adversarial robustness against PGD-20 attack and BPDA attack (ICML 2018 best paper). The results in Table 5 demonstrate that PDA has the best clean accuracy outperforming the other methods. Besides, it can be observed that Gaussian noise augmentation has little improvement on adversarial robustness as the image sizes increase on ImageNet.

Table 5. The results of adversarial robustness for AlexNet on ImageNet. PDA has comparable adversarial robustness and better clean accuracy than its counterparts.

AlexNet	Clean	PGD-20 Attack ($\epsilon=8$)	BPDA Attack ($\epsilon=8$)
Natural	59.08%	2.40%	7.90%
PGD-10-2 [24]	53.30%	25.20%	26.80%
GDA-0.4 [12]	43.42%	1.67%	1.02%
PDA-3-10	56.76%	27.40%	28.20%

5.3. Corruption Robustness

In addition to the adversarial examples of worst-case bounded perturbations, we further test more general sets of corruptions that are likely to encounter in real-world settings. Similar to the benchmark [16], we divide all 15 corruptions into 4 sets: *Noise*, *Blur*, *Weather* and *Digital*. Table 6 compares the performances of our proposed PDA and other methods on CIFAR-10-C and ImageNet-C. On

Table 6. The corruption robustness of naturally trained model and models augmented with different strategies. The table above shows the results of VGG16 on CIFAR-10-C, and the table below represents the results of AlexNet on ImageNet-C. The detailed results are provided in the appendix. PDA has the lowest mCE and corruption errors as well as better clean error than other augmentation strategies.

VGG16	Clean Error	mCE	RmCE	Noise	Blur	Weather	Digital
Naturally Trained	7.48%	100.00%	100.00%	46.22%	30.34%	17.99%	23.64%
PGD-5-1 [24]	12.40%	77.17%	75.57%	18.11%	19.93%	22.67%	25.33%
PGD-10-1 [24]	16.23%	88.29%	85.97%	22.00%	22.02%	26.16%	28.58%
GDA-0.1 [12]	10.86%	76.92%	75.69%	16.39%	25.80%	20.43%	24.97%
GDA-0.4 [12]	31.45%	151.32%	146.47%	25.86%	49.01%	43.86%	47.57%
PDA-3-1.0	9.06%	66.55%	65.56%	18.88%	18.05%	17.90%	20.18%
PDA-3-2.0	10.44%	70.35%	69.10%	15.99%	18.85%	20.77%	21.95%

AlexNet	Clean Error	mCE	RmCE	Noise	Blur	Weather	Digital
Naturally Trained	40.92%	100.00%	100.00%	81.89%	66.95%	71.21%	57.48%
PGD-10-2 [24]	56.58%	107.02%	101.62%	86.38%	73.32%	74.59%	62.73%
GDA-0.4 [12]	46.70%	117.55%	118.15%	71.26%	92.62%	84.26%	78.10%
PDA-3-10	43.24%	98.86%	97.68%	80.64%	65.99%	70.76%	56.98%

CIFAR-10-C, PDA significantly surpasses other strategies on corruption robustness, despite that the naturally trained model performs well on *Digital*. On ImageNet-C, PDA performs better in most corruptions but *Noise*. Figure 3 shows the mean corruption error (mCE) and Relative mCE of models trained with different strategies on CIFAR-10-C and ImageNet-C. It can be seen that PDA has generated more varied data with better general robustness.

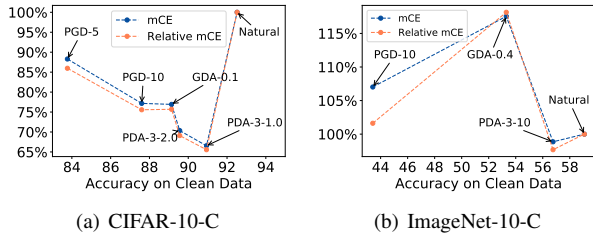


Figure 3. The mCE and Relative mCE of VGG16 on CIFAR-10-C and AlexNet on ImageNet-C. The higher clean accuracy and lower mCE (more lower right) indicate the better general robustness.

5.4. Robustness in the Frequency-based analysis

To better understand the performance of PDA, we conduct the experiment with frequency-based analysis using the method proposed in [38]. First, we perturb each image with noise sampled at each direction and frequency in Fourier domain. Then, we evaluate natural and augmented models with the Fourier-noise-corrupted images and obtain the test errors. Finally, we present the changes of error rates with heat map in Figure 4 and 5, both indicating the model sensitivity to different frequencies and orientation perturbations in the Fourier space. For CIFAR-10 and ImageNet, we add noise with 10% of each image’s norm.

The results show different sensitivities for naturally trained and augmented models. On CIFAR-10, the naturally

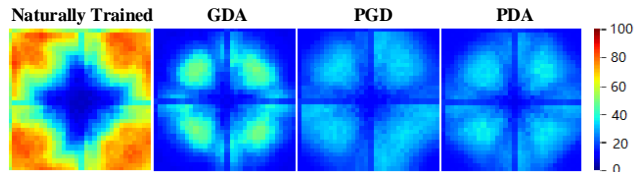


Figure 4. The heat map of model test errors with images perturbed by Fourier basis vectors using different strategies on CIFAR-10.

trained model is sensitive to the high frequencies, where augmentation methods improve robustness with less sacrifice of lower frequencies. We notice that PDA and PGD are less sensitive in lower frequency area than GDA, and PDA appears evenly robust due to the varied data in augmentation. On ImageNet, GDA has little improvement on robustness to higher frequencies (which may need stronger additive noise); in contrast, the PDA-based model improves robustness for both lower and higher frequency noise. Figure 6 shows that, in some cases, adding Fourier-noise with large norm on images is similar to the black-box adversarial attacks, which can preserve the content but mislead the models.

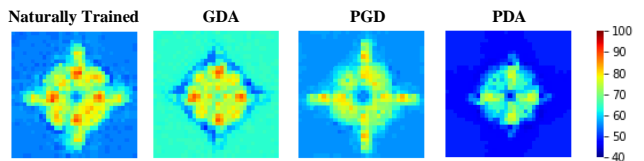


Figure 5. The heat map of model test errors with images perturbed by Fourier basis vectors using different strategies on ImageNet.

5.5. Mixed Test for Generalization Ability

As indicated in [37], if the test data is similar to training data, then the corresponding test error should be close to the empirical training error. Previous adversarial related

studies [1, 36] usually evaluate the accuracy of model on individual type of examples. However, for models trained on dataset augmented with noises, it can be prejudiced to evaluate model generalization ability on the specified type of test data different from the training set. Therefore, it is reasonable to evaluate model generalization ability with mixed types of samples when the model is trained with data augmentation containing noises. Thus, we propose *Mixed Test* to fairly evaluate the model generalization ability of the proposed PDA method. Specifically, the test data combines clean, adversarial and corrupted examples in an equal proportion.

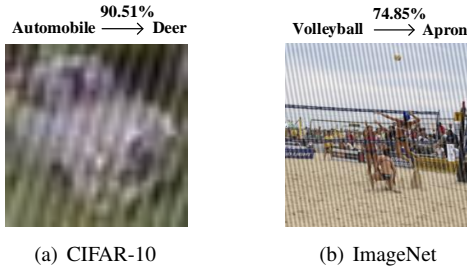


Figure 6. Example images perturbed by Fourier basis vectors with large norm, which misleads model successfully and preserves the content.

The experimental results using *Mixed Test* on CIFAR-10 are shown in Table 7, where ‘C’ denotes clean images, $\epsilon 4$ means the adversarial examples, *Other* = {*Weather*, *Digital*} represents the corruptions mentioned above. See results of SVHN in the appendix. As can be observed, PDA outperforms the other data augmentation methods in terms of the generalization ability. As illustrated in Figure 1, although PGD and GDA increase model robustness against specific noise, they miss some portions of benign examples, thus leading to weaker generalization ability.

Table 7. The results of mixed test with VGG16 on CIFAR-10. PDA performs comprehensively well on mixed test, which confirms the superior general robustness of PDA.

VGG16	C+ $\epsilon 4$ +Blur	C+ $\epsilon 4$ +Noise	C+ $\epsilon 4$ +Other
Natural	60.53%	57.27%	63.69%
PGD-10-1 [24]	75.40%	75.71%	75.69%
GDA-0.1 [12]	71.00%	72.95%	72.87%
PDA-3-1.0	79.75%	80.43%	80.48%

5.6. Effects of Progressive Iterations

The multiple progressive iterations of PDA help improve the noise diversity for augmented models. To further investigate the effect of progressive iterations, we conduct an experiment on PDA with different iterative step k from 1 to 6. As shown in Figure 7, the model robustness drops as the clean accuracy increases, indicating a trade-off between accuracy and robustness. Despite that the larger k brings more

data complexities in the augmentation as ϵ is fixed, it leads to more training time and less improvement on robustness. Therefore, in practice, we set $k=3$ in order to keep the balance between robustness, accuracy and computation cost.

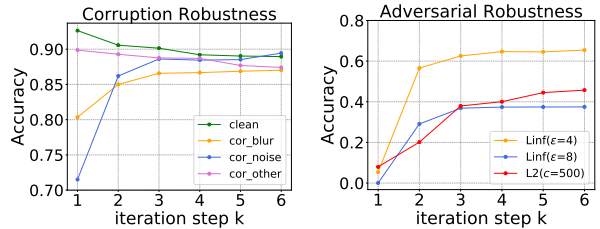


Figure 7. The corruption and adversarial robustness evaluation of PDA on CIFAR-10, where the range of k is from 1 to 6.

5.7. Feature Alignment with Human Vision

Beyond measuring the performance with quantitative results, we also try to discover model robustness more perceptually with visualization techniques. Since the model with stronger adversarial robustness generates gradients that are better aligned with human visual perception [35], we normalize and visualize the gradient of loss w.r.t the input images on CIFAR-10. In Figure 8, the gradients for ‘Natural’ model are noisy and thus appear meaningless to human, while those for PGD and GDA are less perceptually aligned with human vision such as fewer outlines. In contrast, PDA aligns the best to human visual perception.

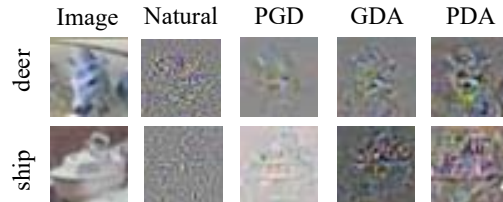


Figure 8. Visualization of the gradients with respect to the input images via different training strategies on CIFAR-10.

6. Conclusions

In this paper, we have proposed a more general augmentation method, *i.e.* the Progressive Data Augmentation (PDA), which adds diversified adversarial noises progressively during training and intends to obtain more general robustness against both adversarial attacks and corruptions. Moreover, PDA has less negative impacts on clean accuracy and cheaper computation cost. We have also theoretically proved the perturbation bound and the generalization ability of PDA. With the frequency-based analysis, we have found that the model trained with PDA is more evenly robust to all kinds of frequencies. We have also noticed that

the model trained with PDA has better generalization ability as evaluated more fairly on the mixed dataset. Experimental evaluations on CIFAR-10, SVHN, ImageNet have demonstrated that PDA performs comprehensively well on adversarial attacks and clean images, having achieved state-of-the-art corruption robustness on the CIFAR-10-C and ImageNet-C benchmarks.

References

- [1] Anish Athalye, Nicholas Carlini, and David Wagner. Obfuscated gradients give a false sense of security: Circumventing defenses to adversarial examples. *arXiv preprint arXiv:1802.00420*, 2018. [2](#), [5](#), [7](#)
- [2] Dzmitry Bahdanau, Kyunghyun Cho, and Yoshua Bengio. Neural machine translation by jointly learning to align and translate. *arXiv preprint arXiv:1409.0473*, 2014. [1](#)
- [3] Yoshua Bengio, Jérôme Louradour, Ronan Collobert, and Jason Weston. Curriculum learning. In *Proceedings of the 26th annual international conference on machine learning*, pages 41–48. ACM, 2009. [4](#)
- [4] J Frédéric Bonnans and Alexander Shapiro. *Perturbation analysis of optimization problems*. Springer Science & Business Media, 2013. [4](#)
- [5] Nicholas Carlini, Anish Athalye, Nicolas Papernot, Wieland Brendel, Jonas Rauber, Dimitris Tsipras, Ian Goodfellow, and Aleksander Madry. On evaluating adversarial robustness. *arXiv preprint arXiv:1902.06705*, 2019. [6](#)
- [6] Nicholas Carlini and David Wagner. Towards evaluating the robustness of neural networks. In *2017 IEEE Symposium on Security and Privacy (SP)*, pages 39–57. IEEE, 2017. [5](#)
- [7] Zachary Charles, Shashank Rajput, Stephen Wright, and Dimitris Papailiopoulos. Convergence and margin of adversarial training on separable data. *arXiv preprint arXiv:1905.09209*, 2019. [3](#)
- [8] Jia Deng, Wei Dong, Richard Socher, Li-Jia Li, Kai Li, and Li Fei-Fei. Imagenet: A large-scale hierarchical image database. In *Computer Vision and Pattern Recognition, 2009. CVPR 2009. IEEE Conference on*, pages 248–255. Ieee, 2009. [2](#), [5](#)
- [9] Samuel Dodge and Lina Karam. A study and comparison of human and deep learning recognition performance under visual distortions. In *2017 26th international conference on computer communication and networks (ICCCN)*, pages 1–7. IEEE, 2017. [2](#)
- [10] Alhussein Fawzi, Hamza Fawzi, and Omar Fawzi. Adversarial vulnerability for any classifier. In *Advances in Neural Information Processing Systems*, pages 1178–1187, 2018. [2](#)
- [11] Alhussein Fawzi, Seyed-Mohsen Moosavi-Dezfooli, and Pascal Frossard. Robustness of classifiers: from adversarial to random noise. In *Advances in Neural Information Processing Systems*, pages 1632–1640, 2016. [2](#)
- [12] Nic Ford, Justin Gilmer, Nicolas Carlini, and Dogus Cubuk. Adversarial examples are a natural consequence of test error in noise. *arXiv preprint arXiv:1901.10513*, 2019. [2](#), [3](#), [5](#), [6](#), [7](#), [8](#)
- [13] Ian J Goodfellow, Jonathon Shlens, and Christian Szegedy. Explaining and harnessing adversarial examples. *arXiv preprint arXiv:1412.6572*, 2014. [2](#)
- [14] Ian J Goodfellow, Jonathon Shlens, and Christian Szegedy. Explaining and harnessing adversarial examples. *arXiv preprint arXiv:1412.6572*, 2014. [3](#)
- [15] Kaiming He, Xiangyu Zhang, Shaoqing Ren, and Jian Sun. Deep residual learning for image recognition. In *Proceedings of the IEEE conference on computer vision and pattern recognition*, pages 770–778, 2016. [5](#)
- [16] Dan Hendrycks and Thomas Dietterich. Benchmarking neural network robustness to common corruptions and perturbations. In *International Conference on Learning Representations*, 2019. [2](#), [3](#), [5](#), [6](#)
- [17] Geoffrey Hinton, Li Deng, Dong Yu, George E. Dahl, Abdelrahman Mohamed, Navdeep Jaitly, Andrew Senior, Vincent Vanhoucke, Patrick Nguyen, and Tara N. Sainath. Deep neural networks for acoustic modeling in speech recognition: The shared views of four research groups. *IEEE Signal Processing Magazine*, 29(6):82–97, 2012. [1](#)
- [18] Alex Krizhevsky and Geoffrey Hinton. Learning multiple layers of features from tiny images. Technical report, Cite-seer, 2009. [2](#), [5](#)
- [19] Alex Krizhevsky, Ilya Sutskever, and Geoffrey E. Hinton. Imagenet classification with deep convolutional neural networks. In *International Conference on Neural Information Processing Systems*, pages 1097–1105, 2012. [1](#), [5](#)
- [20] Alexey Kurakin, Ian Goodfellow, and Samy Bengio. Adversarial examples in the physical world. *arXiv preprint arXiv:1607.02533*, 2016. [2](#), [3](#)
- [21] Alexey Kurakin, Ian Goodfellow, and Samy Bengio. Adversarial machine learning at scale. In *International Conference on Learning Representations*, 2017. [2](#)
- [22] Aishan Liu, Xianglong Liu, Jiabin Fan, Yuqing Ma, Anlan Zhang, Huiyuan Xie, and Dacheng Tao. Perceptual-sensitive gan for generating adversarial patches. In *33rd AAAI Conference on Artificial Intelligence*, 2019. [2](#)
- [23] Raphael Gontijo Lopes, Dong Yin, Ben Poole, Justin Gilmer, and Ekin D Cubuk. Improving robustness without sacrificing accuracy with patch gaussian augmentation. *arXiv preprint arXiv:1906.02611*, 2019. [2](#)
- [24] Aleksander Madry, Aleksandar Makelev, Ludwig Schmidt, Dimitris Tsipras, and Adrian Vladu. Towards deep learning models resistant to adversarial attacks. *arXiv preprint arXiv:1706.06083*, 2017. [2](#), [3](#), [5](#), [6](#), [7](#), [8](#)
- [25] Luke Metz, Niru Maheswaranathan, Jonathon Shlens, Jascha Sohl-Dickstein, and Ekin D Cubuk. Using learned optimizers to make models robust to input noise. *arXiv preprint arXiv:1906.03367*, 2019. [2](#)
- [26] Yuval Netzer, Tao Wang, Adam Coates, Alessandro Bisacco, Bo Wu, and Andrew Y Ng. Reading digits in natural images with unsupervised feature learning. 2011. [2](#), [5](#)
- [27] Swami Sankaranarayanan, Arpit Jain, Rama Chellappa, and Ser Nam Lim. Regularizing deep networks using efficient layerwise adversarial training. In *Thirty-Second AAAI Conference on Artificial Intelligence*, 2018. [2](#)

- [28] Ludwig Schmidt, Shibani Santurkar, Dimitris Tsipras, Kunal Talwar, and Aleksander Madry. Adversarially robust generalization requires more data. In *Advances in Neural Information Processing Systems*, pages 5014–5026, 2018. [2](#), [3](#)
- [29] Ali Shafahi, Mahyar Najibi, Amin Ghiasi, Zheng Xu, John Dickerson, Christoph Studer, Larry S Davis, Gavin Taylor, and Tom Goldstein. Adversarial training for free! *arXiv preprint arXiv:1904.12843*, 2019. [2](#), [5](#), [6](#)
- [30] Uri Shaham, Yutaro Yamada, and Sahand Negahban. Understanding adversarial training: Increasing local stability of supervised models through robust optimization. *Neurocomputing*, 307:195–204, 2018. [3](#)
- [31] Karen Simonyan and Andrew Zisserman. Very deep convolutional networks for large-scale image recognition. *arXiv preprint arXiv:1409.1556*, 2014. [5](#)
- [32] Aman Sinha, Hongseok Namkoong, and John Duchi. Certifiable distributional robustness with principled adversarial training. *stat*, 1050:29, 2017. [2](#), [3](#)
- [33] Ke Sun, Zhanxing Zhu, and Zhouchen Lin. Towards understanding adversarial examples systematically: Exploring data size, task and model factors. *arXiv preprint arXiv:1902.11019*, 2019. [2](#), [3](#)
- [34] Zhun Sun, Mete Ozay, Yan Zhang, Xing Liu, and Takayuki Okatani. Feature quantization for defending against distortion of images. In *Proceedings of the IEEE Conference on Computer Vision and Pattern Recognition*, pages 7957–7966, 2018. [2](#)
- [35] Dimitris Tsipras, Shibani Santurkar, Logan Engstrom, Alexander Turner, and Aleksander Madry. Robustness may be at odds with accuracy. *stat*, 1050:11, 2018. [8](#)
- [36] Cihang Xie, Jianyu Wang, Zhishuai Zhang, Zhou Ren, and Alan Yuille. Mitigating adversarial effects through randomization. In *International Conference on Learning Representations*, 2018. [2](#), [7](#)
- [37] Huan Xu and Shie Mannor. Robustness and generalization. *Machine learning*, 86(3):391–423, 2012. [4](#), [7](#)
- [38] Dong Yin, Raphael Gontijo Lopes, Jonathon Shlens, Ekin D Cubuk, and Justin Gilmer. A fourier perspective on model robustness in computer vision. *arXiv preprint arXiv:1906.08988*, 2019. [7](#)
- [39] Runtian Zhai, Tianle Cai, Di He, Chen Dan, Kun He, John Hopcroft, and Liwei Wang. Adversarially robust generalization just requires more unlabeled data. *arXiv preprint arXiv:1906.00555*, 2019. [3](#)
- [40] Dinghui Zhang, Tianyuan Zhang, Yiping Lu, Zhanxing Zhu, and Bin Dong. You only propagate once: Accelerating adversarial training via maximal principle. *arXiv preprint arXiv:1905.00877*, 2019. [2](#), [5](#), [6](#)
- [41] Stephan Zheng, Yang Song, Thomas Leung, and Ian Goodfellow. Improving the robustness of deep neural networks via stability training. In *IEEE conference on computer vision and pattern recognition*, 2016. [2](#)